一般セッション(口頭講演) | 10 スピントロニクス・マグネティクス：10.4 半導体・トポロジカル・超伝導・強相関スピントロニクス

2025年3月17日(月) 13:30 ~ 16:45 K102 (講義棟)

[17p-K102-1~12] 10.4 半導体・トポロジカル・超伝導・強相関スピントロニクス

岡林 潤(東大)、 ファム ナムハイ(科学大)

英語発表

13:30 ~ 13:45

[17p-K102-1]

[The 57th Young Scientist Presentation Award Speech] Control of the valley lifetime in a suspended WSe_2 monolayer by opto-electro-mechanical tuning

○Giacomo Mariani[1], Yoji Kunihashi[1], Louis Smet[1], Taro Wakamura[1], Satoshi Sasaki[1], Jun Ishihara[2], Makoto Kohda[2], Junsaku Nitta[1,2], Haruki Sanada[1] (1.NTT-BRL, 2.Tohoku Univ.)

奨励賞エントリー 英語発表

13:45 ~ 14:00

[17p-K102-2]

Novel method for optical evaluation of persistent spin helix state in a GaAs/AlGaAs two-dimensional electron gas

○Keito Kikuchi[1], Jun Ishihara[1], Miari Hiyama[1], Sota Yamamoto[1], Yuzo Ohno[2], Makoto Kohda[1,3,4,5] (1.Grad. Sch. of Eng., Tohoku Univ., 2.Univ. of Tsukuba, 3.CSIS, Tohoku Univ., 4.DEFS, Tohoku Univ., 5.QUARC, QST)

奨励賞エントリー 英語発表

14:00 ~ 14:15

[17p-K102-3]

Giant Spin-Orbit Torque in a Two-Dimensional Hole Gas at the Surface of Hydrogen-Terminated Diamond

○Fujio Sako[1], Ryo Ohshima[1,2], Yuichiro Ando[3], Naoya Morioka[2,4], Hiroyuki Kawashima[4], Riku Kawase[4], Norikazu Mizuochi[2,4], Hans Huebl[5,6,7], Masashi Shiraishi[1,2] (1.Kyoto Univ., 2.CSRN, Kyoto Univ., 3.Osaka Metro. Univ., 4.ICR, Kyoto Univ., 5.W.-Meissner-Inst., 6.Tech. Univ. Munich, 7.Munich CQST)

英語発表

14:15 ~ 14:30

[17p-K102-4]

Observation of Nonreciprocal Transport in Two-Dimensional Hole Gas at the Surface of Hydrogen-Terminated Diamond Surface

○Fujio Sako[1], Ryo Ohshima[1,2], Yuichiro Ando[3], Naoya Morioka[2,4], Hiroyuki Kawashima[4], Riku Kawase[4], Norikazu Mizuochi[2,4], Masashi Shiraishi[1,2] (1.Kyoto Univ., 2.CSRN, Kyoto Univ., 3.Osaka Metro. Univ., 4.ICR, Kyoto Univ.)

14:30 ~ 14:45

[17p-K102-5]

(110)GaAs/AlGaAs 量子井戸における電子スピン緩和機構の定量的考察

○大野 裕三[1,2]、揖場 聡[2] (1.筑波大数理、2.産総研)

奨励賞エントリー 英語発表

14:45 ~ 15:00

[17p-K102-6]

Thickness-dependent magnetization switching induced by spin-orbit torque in Weyl ferromagnet $SrRuO_3$ single-layer films

○(D)Hiroto Horiuchi[1], Wakabayashi Yuki K.[2], Araki Yasufumi[3], Ieda Jun'ichi[3], Yamanouchi Michihiko[4], Kaneta-Takada Shingo[1], Taniyasu Yoshitaka[2], Yamamono Hideki[2], Krockenberger Yoshiharu[2], Tanaka Masaaki[1,5], Ohya Shinobu[1,5] (1.The Univ. of Tokyo, 2.NTT BRL, 3.JAEA, 4.Hokkaido Univ., 5.CSRN)

🏷 奨励賞エントリー 🏷 英語発表

15:15 ~ 15:30

[17p-K102-7]

Low current operation of silicon spin devices

○Yasuyuki Koshino[1], Minori Goto[2], Ryo Ohshima[3], Masashi Shiraishi[3], Yuichiro Ando[1,4] (1.Osaka Metropolitan Univ., 2.Univ, of Fukui, 3.Kyoto Univ., 4.JST PRESTO)

🏷 奨励賞エントリー 🏷 英語発表

15:30 ~ 15:45

[17p-K102-8]

Generation of highly spin-polarized electrons in Si at room temperature using low-resistance CoFe/Fe/Mg/MgO/n^+-Si junctions

○(B)Ryosuke Shimizu[1], Shoichi Sato[1,2], Masaaki Tanaka[1,2,3], Ryosho Nakane[1,3,4] (1.EEIS, 2.CSRN, 3.NanoQuine, 4.d.lab)

🏷 奨励賞エントリー 🏷 英語発表

15:45 ~ 16:00

[17p-K102-9]

Optimized growth condition and quantum oscillation of topological semimetal Sb

○Tomoki Hotta[1], Le Duc Anh[1,2], Masaaki Tanaka[1,2] (1.Univ. of Tokyo, 2.CSRN, Univ. of Tokyo)

🏷 奨励賞エントリー 🏷 英語発表

16:00 ~ 16:15

[17p-K102-10]

Effect of Pt and Bi on the spin Hall angle in topological semimetal YPtBi

○Sho Kagami[1], Ohiro Fujie[1], Daiki Ito[1], Quang Le[2], Brian York[2], Cherngye Hwang[2], Xiaoyong Liu[2], Son Le[2], Maki Maeda[3], Tuo Fan[3], Yu Tao[3], Hisashi Takano[3], Pham Nam Hai[1] (1.Institute of Science Tokyo, 2.Western Digital Inc., Great Oaks, 3.Western Digital Inc., Fujisawa)

🏷 奨励賞エントリー 🏷 英語発表

16:15 ~ 16:30

[17p-K102-11]

Superconductivity of In-doped α-Sn thin films grown by molecular beam epitaxy

○Keidai Toyoshima[1], Hideki Maki[1], Le Duc Anh[1,2], Masaaki Tanaka[1,2] (1.Univ. of Tokyo, 2.CSRN, Univ. of Tokyo)

🏷 英語発表

16:30 ~ 16:45

[17p-K102-12]

Detailed investigation of field-free superconducting diode effect in layered superconductor FeSe

○(M1)Utane Nagata[1], Akito Daido[3,2], Ryo Ohshima[1,2], Youichi Ynanase[2,3], Masashi Shiraishi[1,2]
(1.Dept. of Engineering, Kyoto Univ., 2.CSRN Kyoto Univ., 3.Dept. of Science, Kyoto Univ.)

Control of the valley lifetime in a suspended WSe_2 monolayer by opto-electro-mechanical tuning

NTT 物性基礎研 [1], 東北大院工 [2], ○G. Mariani[1], 国橋 要司 [1], L. Smet[1], 若村 太郎 [1], 佐々木 智 [1], 石原 淳 [2], 好田 誠 [2], 新田 淳作 [1,2], 眞田 治樹 [1]

NTT-BRL[1], Tohoku Univ.[2], ○G. Mariani[1], Y. Kunihashi[1], L. Smet[1], T. Wakamura[1], S. Sasaki[1], J. Ishihara[2], M. Kohda[2], J. Nitta[1,2] and H. Sanada[1]

E-mail: giacomo.mariani@ntt.com

Two-dimensional (2D) transition-metal dichalcogenides (TMD) are emerging materials which exhibit novel physical phenomena related to their valley degree of freedom. Access and control of the valley information is challenging due to lattice defects, external contaminations, and contact with other materials which degrade the properties of 2D TMD and limit their tunability; monolayers suspended over empty spaces are an alternative. The contact-free nature of the suspended monolayers enables a precise control of the intrinsic valley lifetime and in future may unlock hidden valley phenomena.

Here, we report that the lifetime of the valley polarization can be controlled by tuning the optical, electrical, and mechanical properties of a suspended and undoped WSe_2 monolayer. In previous studies related to suspended monolayers, photoluminescence spectroscopy was used to probe bright and short-lived exciton dynamics as a function of the monolayer deflection produced by electrostatic gating [1]. However, since photoluminescence gives only a limited overview of the carrier dynamics, it does not reveal the contribution of neither "resident" carriers nor non-radiative excitonic species which are expected to have valley lifetimes on the order of nano- and micro-seconds [2]. In our study, we measured the valley polarization of a suspended monolayer by using a two-color and time-resolved Kerr rotation spectroscopy which allowed us to discuss the long lifetime of the valley polarization given by charged resident carriers as a function of a gate voltage V_g applied to the device shown in Fig. 1(a). Moreover, we strategically designed the mechanical, optical, and electrical parameters of our device to optimize the signal-to-noise ratio of the Kerr rotation spectroscopy conducted at a temperature of 7 K. As a result, we realized the control of the valley lifetime in range of 1-100 ns (Fig. 1(b)) by electrostatic gating in a low doping ($< 2 \cdot 10^{11}$ cm^{-2}) and strain (< 0.2 %) regime of the material [3]. The suspended configuration allowed us to exclude the influence of photo-charged defects at the interface which were previously shown to affect the Kerr rotation signal in encapsulated monolayers.

As a next step after these experiments, we have further improved our fabrication techniques to reduce the influence of other factors such as lattice defects or strain puddles on the intrinsic carrier dynamics in suspended monolayers. The obtained suspended WSe_2 monolayers have large area for optical access, high degree of tunability, and reduced spatial inhomogeneities compared to the monolayers directly exfoliated on substrates by using tape. Our goal is to obtain suspended monolayers with optical homogeneous linewidths which are expected to clearly answer open questions about valley dynamics and empower valley physics in TMD monolayers.

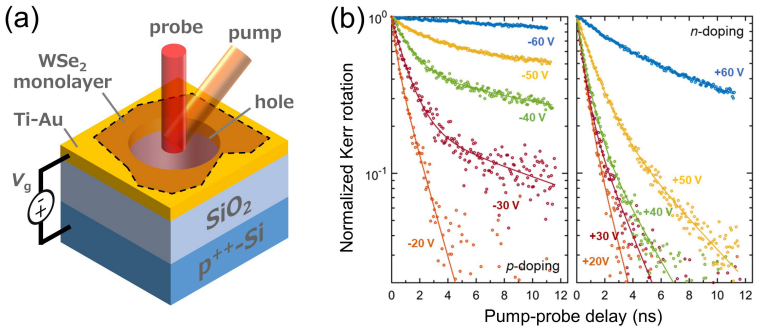

Fig.1: (a) Sketch of the device structure with the suspended monolayer. (b) Time-resolved Kerr rotation as a function of the gate voltage V_g.

References

[1] P. Hernández López, *et al.*, Nat. Commun. **13**(1), 7691 (2022).
[2] J. Li, *et al.*, Phys. Rev. Mater. **5**, 044001 (2021).
[3] G. Mariani, *et al.*, Appl. Phys. Lett. **125**(25), 252401 (2024).

Novel method for optical evaluation of persistent spin helix state in a GaAs/AlGaAs two-dimensional electron gas

Grad. Sch. of Eng., Tohoku Univ.[1], Univ. of Tsukuba[2], CSIS, Tohoku Univ.[3], DEFS, Tohoku Univ.[4], and QUARC, QST[5]

○K. Kikuchi[1], J. Ishihara[1], M. Hiyama[1], S. Yamamoto[1], Y. Ohno[2], and M. Kohda[1,3-5]

Email: keito.kikuchi.t5@dc.tohoku.ac.jp

We propose and demonstrate a novel method for the evaluation of persistent spin helix (PSH) states, where spin states are conserved for a long time in nonmagnetic materials [1]. The PSH state occurs when the contributions of spin-orbit interactions (SOI), Rashba-type and Dresselhaus-type, are equal. Under these conditions, spins form a helical spatial structure (spin helix) that is less susceptible to relaxation caused by scattering. Spin helix is gaining attention as a novel information carrier in spintronics devices, as its wavelength, amplitude, and phase can be utilized for storing, transferring, and manipulating information [2]. However, conventional methods for evaluating SOI parameters often require sample processing and external magnetic fields, making the experimental setup complex and the measurements cumbersome.

In this study, we address these issues by combining time-resolved Kerr rotation (TRKR) measurement with a spatial light modulator (SLM). The SLM is used to spatially modulate the polarization of the pump pulse to generate a spin helix of any desired single wavenumber. Meanwhile, a probe pulse is employed to measure the temporal dynamics of the spin polarization density with high precision [3]. This combination allows efficient analysis of the spin helix relaxation rate without requiring spatial scanning or external magnetic fields.

The experiments were conducted using a (001)-oriented 20 nm GaAs/AlGaAs quantum well structure. Figure 1 illustrates the temporal dynamics of the spin polarization density at the center of spin helices excited using the SLM. The results indicate that relaxation characteristics vary significantly depending on the wavenumbers. Figure 2 presents the wavenumber dependence of the relaxation rate. The relaxation rate follows a parabolic trend as a function of wavenumber, expressed as $\Gamma = D_s(q_x - q_0)^2 + \frac{1}{\tau_0}$, where $q_0 = \frac{2m^*}{\hbar^2}(-\alpha + \beta)$ and $\frac{1}{\tau_0} = \frac{2D_s m^{*2}}{\hbar^4}[(\alpha+\beta)^2 + 3\beta_3^2]$. The SOI parameters ($\alpha$, β_1, β_3) and spin diffusion coefficient (D_s) were determined from the minimum of the parabola and its curvature. These results indicate that the present method, which combines SLM and TRKR measurement, can efficiently and conveniently evaluate the relaxation dynamics of spin helices in the PSH state.

This research was supported by JSPS KAKENHI Grant No. 21H04647 and JST FOREST, CREST, PRESTO, and SPRING programs (Grant Nos. JPMJFR203C, JPMJCR22C2, JPMJPR24L4, and JPMJSP2114).

[1] M. P. Walser *et al.,* Nat. Phys. **8**, 757 (2012).
[2] M. Kohda *et al.,* Appl. Phys. Lett. **123**, 190502 (2023).
[3] K. Kikuchi *et al*., arXiv:2411.10963 (2024).

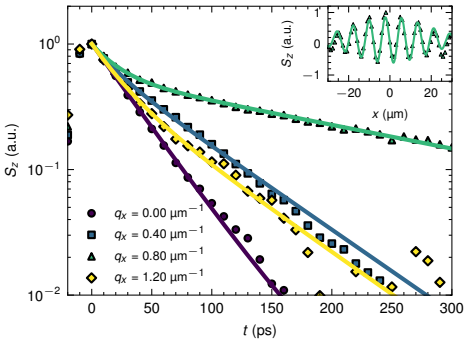

Fig 1: Temporal dynamics of the spin polarization density at $x = 0$, $S_z(t) = A\exp(-\Gamma t)$, each characterized by a different wavenumber, excited using the SLM. The inset in the upper-right corner shows the spatial distribution of the spin helix with $q_x = 0.80$ μm^{-1} at $t = 0$ ps, where $x||[1\bar{1}0]$.

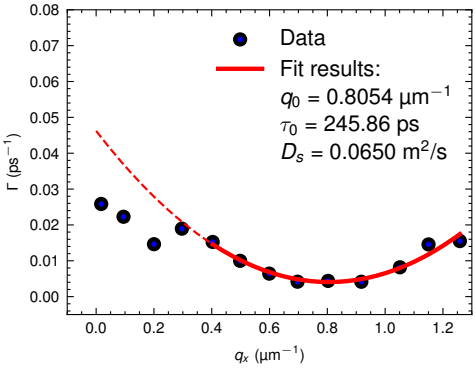

Fig 2: Wavenumber dependence of the relaxation rate extracted from the temporal dynamics of spin helices.

Giant Spin-Orbit Torque in a Two-Dimensional Hole Gas at the Surface of Hydrogen-Terminated Diamond

Kyoto Univ.[1], Center for Spintronics Research Network, Kyoto Univ.[2], Osaka Metropolitan Univ.[3], Institute for Chemical Research, Kyoto Univ.[4], Walther-Meissner-Institute[5], Technical University of Munich[6], Munich Center for Quantum Science and Technology[7],

◦Fujio Sako[1], Ryo Ohshima[1,2], Yuichiro Ando[3], Naoya Morioka[2,4], Hiroyuki Kawashima[4], Riku Kawase[4], Norikazu Mizuochi[2,4], Hans Huebl[5,6,7] and Masashi Shiarishi[1,2]

E-mail: sako.fujio.26z@st.kyoto-u.ac.jp

Two-dimensional hole gas (2DHG) is created at the surface of hydrogen-terminated (H-) diamond, which has been intensively studied as a field effect transistor [1]. In addition, the inner electric field perpendicular to the carrier plane induces the strong Rashba-type spin-orbit coupling [2], which leads to possible charge-to-spin conversion through the Rashba-Edelstein effect. In this study, the charge-to-spin conversion in H-diamond was observed by performing the second harmonic Hall measurement, which is a potential technique to estimate spin-orbit torque (SOT) efficiency [3].

A Hall-bar shaped H-diamond (001) / $Ni_{80}Fe_{20}$ (Py) device was prepared by using e-beam lithography and e-beam deposition, and the transverse second harmonic voltage was measured at room temperature (RT) under the application of an alternative current and an in-plane magnetic field H_{ext} with angle φ (see Fig. 1). The SOT efficiency ξ_{DL} was investigated from φ and H_{ext} dependence of transverse second harmonic voltage. The ξ_{DL} is negative at the samples with thin Py (≦ 5 nm) due to SOT from the 2DHG, and it is positive at the samples with thicker Py (≧ 7 nm) because self-induced SOT in Py becomes dominant in thick Py layer (see Fig. 2). The Rashba-Edelstein length in the 2DHG λ_{REE}^{2DHG}, which is equivalent to the inverse Rashba-Edelstein length λ_{IREE} or the product of spin Hall angle θ and spin diffusion length λ_s, was estimated as an index of the charge to spin conversion efficiency in 2DHG. The estimation of λ_{REE}^{2DHG} was implemented by solving the spin diffusion equation, in which the 2DHG is considered as the boundary condition for the Py, i.e., the spin-dependent chemical potential at the bottom of the Py layer is set to be $E\lambda_{REE}^{2DHG}$, where E is the electric field generated by the applied AC current. The theoretical fitting curve as well is shown in Fig.2, and λ_{REE}^{2DHG} is estimated to be -0.19 ± 0.07 nm, which is comparable to $\theta\lambda_s$ of Pt (0.05 nm [4] at RT) and λ_{IREE} in $LaAlO_3$ / $SrTiO_3$ (0.2 nm at RT [5]). The sign reversal of ξ_{DL} for the t_{Py} was not observed in the sample of oxygen-terminated (O-) diamond / Py, because O-diamond does not host 2DHG on its surface, which is the supporting evidence of the successful observation of the efficient spin conversion in the 2DHG.

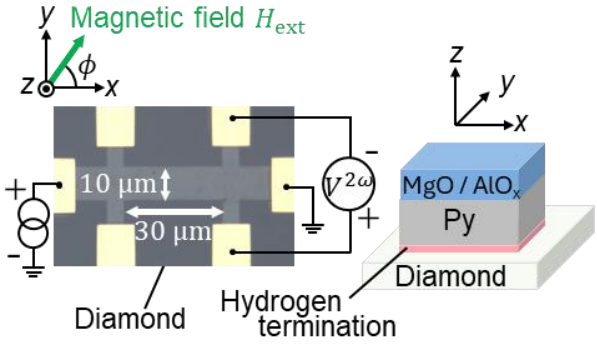

Figure 1: Device structure and measurement setup.

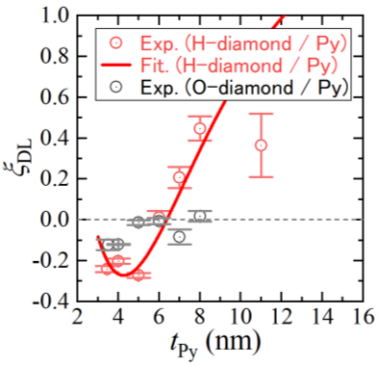

Figure 2: Py thickness dependence of SOT efficiency in H- (O-) diamond / Py samples.

[1] Y. Sasama *et al., Nat. Electron.* **5**, 37 (2022). [2] G. Akhgar *et al., Nano Lett.* **16**, 3768 (2016).
[3] F. Sako *et al., Phys. Rev. B* **110**, L220407 (2024). [4] E. Sagasta *et al., Phys. Rev. B* **94**, 060412(R) (2016).
[5] J.-Y. Chauleau *et al., Europhys. Lett.* **116**, 17006 (2016).

Observation of Nonreciprocal Transport in Two-Dimensional Hole Gas at the Surface of Hydrogen-Terminated Diamond Surface

Kyoto Univ.[1], Center for Spintronics Research Network, Kyoto Univ.[2],

Osaka Metropolitan Univ.[3], Institute for Chemical Research, Kyoto Univ.[4],

◦Fujio Sako[1], Ryo Ohshima[1,2], Yuichiro Ando[3], Naoya Morioka[2,4],

Hiroyuki Kawashima[4], Riku Kawase[4], Norikazu Mizuochi[2,4] and Masashi Shiarishi[1,2]

E-mail: sako.fujio.26z@st.kyoto-u.ac.jp

Hydrogen-terminated (H-) diamond (Fig. 1) hosts two-dimensional hole gas (2DHG) at its surface. The triangular potential at the surface gives rise to sizable Rashba-type spin splitting in the *E-k* dispersion [1] in the system consisting of light elements, or C and H. Spin-momentum locking in the Rashba-type band structure results in conversion from an electric current to spin polarization in the transverse direction, which attracts much attention as a means of realizing high-efficiency charge-to-spin conversion. Magnetic moment of the polarized spin interacts with magnetic field, and nonreciprocal transport takes place under an external magnetic field parallel to the spin polarization. In this study, nonreciprocal transport in 2DHG at H-diamond surface was examined.

In the Rashba system, longitudinal resistance R is expressed as $R = R_0\{1 + \gamma B_{ext} I \sin(\varphi)\}$ [2], where γ is a magnitude of the modulation of resistance, B_{ext} is an external magnetic field, I is an electric current, and φ represents the azimuthal angle of an external magnetic field to the electric current. Under the external magnetic field at φ = 90 °, an alternative current $I = I_0 \sin(\omega t)$ induces the second harmonic resistance $R^{2\omega}\cos(2\omega t)$, which is described as

$$R^{2\omega} = -\gamma B_{ext} I_0 / 2. \qquad (1)$$

A Hall-bar shaped H-diamond (001) sample with gold electrodes was prepared by using e-beam lithography and e-beam deposition. A gate voltage V_G was applied by using an ionic gating technique, where an electric double layer can be formed onto the 2DHG. Figure 2a shows the B_{ext} dependence of the $R^{2\omega}$ at 5 K, which was measured under the condition of φ = 90 °and V_G = -1.8 V. The odd component of the $R^{2\omega}$ that is proportional to the B_{ext} is noticeable, which signifies successful observation of the nonreciprocal transport. The slope of the $R^{2\omega}$-B_{ext} characteristic ($R^{2\omega}$ / B_{ext}) is proportional to the I_0 (see Fig. 2b) as expected from Eq. (1). The nonreciprocity is enhanced at lower temperature because thermal fluctuation of spin is suppressed, and γ became the maximum value of 0.22 $A^{-1}T^{-1}$ at 15 K, which is comparable to 0.22 $A^{-1}T^{-1}$ at 2 K in WTe_2 [3] and 0.52 $A^{-1}T^{-1}$ at 1.5 K in InSb / CdTe [4]. The details will be discussed in the presentation.

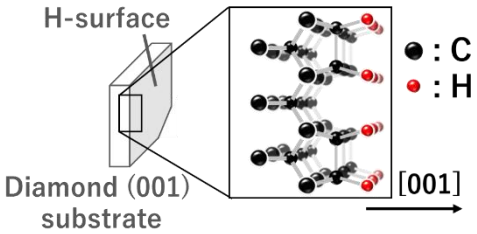

Fig. 1: Structural image of hydrogen-terminated diamond.

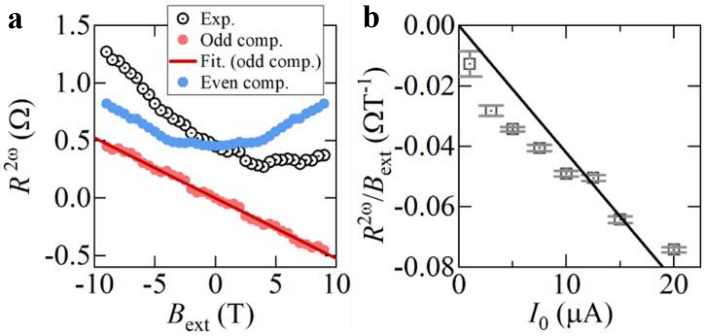

Fig. 2: a) B_{ext} dependence of $R^{2\omega}$. Black open dots are experimental data, and blue / red solid dots are odd- / even-components, respectively. b) I_0 dependence of $R^{2\omega}$ / B_{ext}.

[1] G. Akhgar *et al., Nano Lett.* **16**, 3768 (2016). [2] T. Ideue *et al., Nat. Phys.* **13**, 578 (2017).
[3] P. He *et al., Nat. Commun.* **10**, 1209 (2019). [4] L. Li *et al., Adv. Matt.* **35**, 2207322 (2023).

(110)GaAs/AlGaAs 量子井戸における電子スピン緩和機構の定量的考察

Quantitative consideration of electron spin relaxation mechanisms in (110) GaAs/AlGaAs quantum wells

筑波大数理[1]，産総研[2] ○大野 裕三[1,2]，揖場 聡[2]

Univ. of Tsukuba[1], AIST[2], ○Yuzo Ohno[1,2], Satoshi Iba[2]

E-mail: ono.yuzo.gb@u.tsukuba.ac.jp

Electron spin-relaxation time (τ_s) is a key parameter in semiconductor spintronics. In particular, for devices operating at room temperature, a longer τ_s is expected to enable spin-dependent transport and light emission while preserving the spin state, thus paving the way for semiconductor spin lasers [1,2]. However, the Dresselhaus-type effective magnetic field arising from spin–orbit interactions, due to bulk inversion asymmetry in III–V semiconductor quantum wells (QWs), significantly enhances spin relaxation via the D'yakonov–Perel (DP) mechanism. As a result, τ_s can be shortened to around 100 ps at room temperature, hindering device realization. To address this issue, we have focused on (110)-oriented QWs, in which the effective magnetic field is perpendicular to the QW plane, thereby suppressing out-of-plane spin relaxation via the DP mechanism. Although various spin-relaxation mechanisms operating under suppressed DP conditions have been proposed and τ_s has been discussed qualitatively, it is crucial to quantitatively elucidate the contribution of each mechanism.

In this study, we investigated the impact of different spin-relaxation mechanisms on τ_s in (110) GaAs/AlGaAs QWs. We calculated τ_s as a function of quantized energy, temperature, and electron density, taking into account the Elliott–Yafet (EY), intersubband spin relaxation (ISR), and exciton spin relaxation (ExSR) mechanisms. As shown in Fig. 1, our calculations agree well with the experimental data for (110) QWs. Our analysis revealed that the contribution of each mechanism to τ_s can be quantitatively identified and that the dominant mechanism varies under different conditions. These findings provide guidance for optimizing (110) QW-based spintronic devices and enable precise estimation of τ_s under relevant operating conditions.

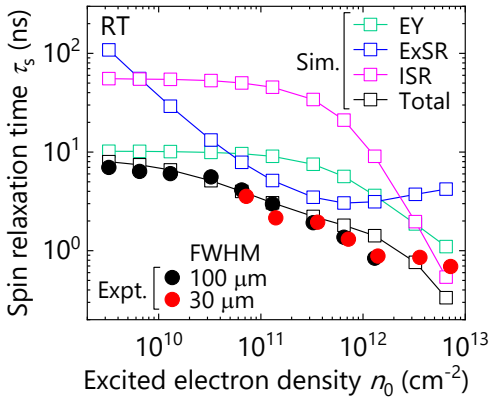

Fig. 1 Excited electron density dependence of spin relaxation time τ_s in undoped (110) GaAs/AlGaAs quantum wells at room temperature. Closed circles and open squares represent the experimental and calculated data, respectively.

This work was supported by JSPS KAKENHI (Grant Number JP24H00426, JP24K01391), and MEXT Initiative to Establish Next-generation Novel Integrated Circuits Centers (X-NICS) (Grant Number JPJ011438).

[1] Y. Ohno et al., Appl. Phys. Express 13, 123003 (2020).
[2] S. Iba et al., Micromachines 12, 1112 (2021).

Thickness-dependent magnetization switching induced by spin-orbit torque in Weyl ferromagnet $SrRuO_3$ single-layer films

○H. Horiuchi[1], Y. K. Wakabayashi[2], Y. Araki[3], J. Ieda[3], M. Yamanouchi[4], S. Kaneta-Takada[1], Y. Taniyasu[2], H. Yamamoto[2], Y. Krockenberger[2], M. Tanaka[1,5] and S. Ohya[1,5]
[1]*Department of Electrical Engineering and Information Systems, The University of Tokyo*
[2]*NTT Basic Research Laboratories, NTT Corporation*
[3]*Advanced Science Research Center, Japan Atomic Energy Agency*
[4]*Division of Electronics for Informatics, Graduate School of Information Science and Technology, Hokkaido University*
[5]*Center for Spintronics Research Network (CSRN), The University of Tokyo*
E-mail: h-horiuchi22@g.ecc.u-tokyo.ac.jp

The Weyl ferromagnet $SrRuO_3$ (SRO) [1–3] holds significant potential for developing energy-efficient spin-orbitronics devices. Recently, we have successfully demonstrated spin-orbit torque (SOT)-induced *partial* magnetization switching in a full-epitaxial high-quality SRO *single* layer [4]. Although the film appears to be seemingly uniform, our detailed analyses revealed the presence of an inhomogeneous distribution of oxygen octahedral rotation (OOR), with particularly pronounced rotation near the SRO/$SrTiO_3$ (STO) interface. The strong spin Berry curvature induced by the OOR generates a significant intrinsic spin Hall effect (SHE), leading to the magnetization reversal in the SRO layer near the SRO/STO interface. This experiment implies that the switching behavior may vary depending on the film thickness; however, there is no systematic thickness-dependent study of the SOT magnetization switching in SRO.

In this study, we grew SRO films with various thicknesses d of 5, 15, and 26 nm on STO (001) substrates using a machine-learning-assisted molecular beam epitaxy system [5]. Partial SOT magnetization switching was observed in all films (red dots in Fig. 1). The chirality of the switching hysteresis loops changes by reversing the sign of the in-plane supporting field applied along the current direction (not shown), confirming that SOT drives the observed magnetization switching. The switching current density was in the order of MA cm^{-2}, one order of magnitude smaller than conventional ferromagnet/heavy metal *bilayer* systems [6], which highlights the potential of SRO for highly efficient switching. The switching ratio, defined as the size of the switching loops (processes 1 and 2 in Fig.1) relative to that of the anomalous Hall effect loops (blue curves in Fig. 1), was found to increase in SRO films with larger d. For example, when d = 15 nm, the switching ratio is approximately 3.5 (=11%/3.1%) times larger than when d = 5 nm. In this presentation, we will also discuss the intriguing polarity reversal of the switching loops for different d.

This work was partly supported by Grants-in-Aid for Scientific Research, JST CREST, JST ERATO, and Spintronics Research Network of Japan (Spin-RNJ).

References: [1] G. Koster *et al*., *Rev. Mod. Phys.* **84**, 253-298 (2012). [2] K. Takiguchi *et al*., *Nat. Commun.* **11**, 4969 (2020). [3] Y. Chen *et al*., *Phys. Rev. B* **88**, 125110 (2013). [4] H. Horiuchi *et al*., arXiv:2411.01806 (2024). [5] Y. Wakabayashi *et al*., *APL Mater.* **7**, 101114 (2019). [6] I. M. Miron *et al*., *Nature* **476**, 189 (2011).

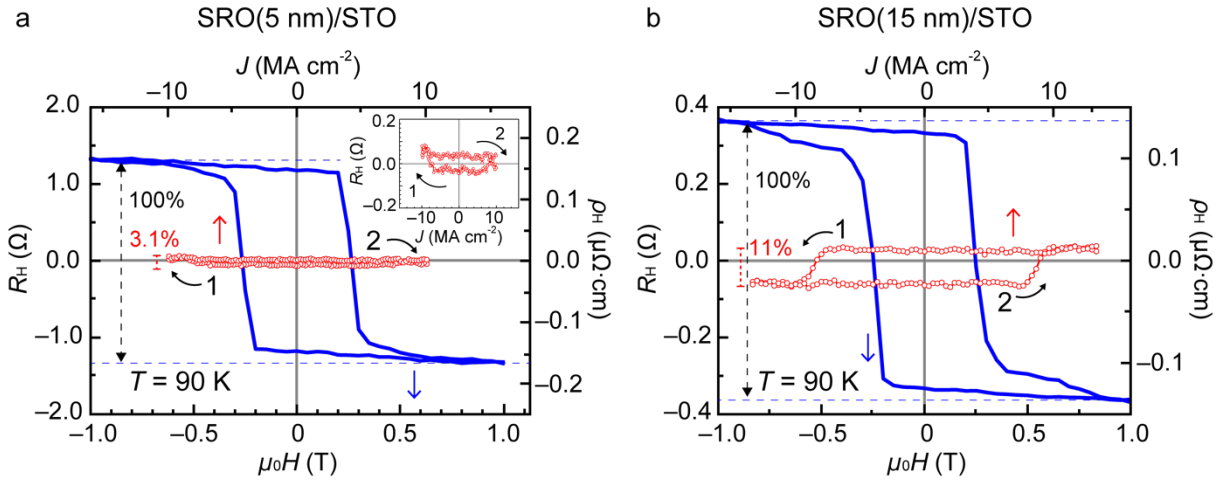

Fig. 1 Anomalous Hall effect (AHE) (blue solid line) and SOT-induced partial magnetization switching (red hollow circles) in (a) SRO (5 nm) and (b) SRO (15 nm) single layers. The switching ratio, indicated in red, was calculated by dividing the saturated value of the SOT switching hysteresis by that of the AHE. The inset shows an enlarged view of the switching loop in (a).

シリコンスピンデバイスの微小電流駆動

Low current operation of silicon spin devices

大阪公大 [1]，福井大 [2]，京大 [3]，JST さきがけ [4]
○(B)越野 靖之 [1]，後藤 穣 [2]，大島 諒 [3]，白石 誠司 [3]，安藤 裕一郎 [1,4]，
Osaka Metropolitan Univ. [1], Univ, of Fukui [2], Kyoto Univ. [3], JST PRESTO[4],
○(B)Yasuyuki Koshino[1], Minori Goto[2], Ryo Ohshima[3], Masashi Shiraishi[3], Yuichiro Ando[1,4]
E-mail: yuichiro.ando@omu.ac.jp

Steady progress has been made in silicon(Si)-based spintronics, including the room temperature demonstration of spin FET[1] and spin XOR logic devices[2], and spin transport in the inversion layer[3]. Since these devices are expected to operate at room temperature, the creation of spin functions at room temperature is a key. Another promising device using spins in Si is quantum computation technology based on Si quantum dots[4]. Recently, a considerably high fidelity has been reported[5], accelerating research and development of Si-based quantum computing. The bottleneck is the detection of the spin state. Currently, Zeeman energy from an external magnetic field is used, but the energy difference that can be formed is small (several tens of μeV) and thus, vulnerable to thermal disturbances. If the ferromagnetic tunnel contacts, established in spin FET, can be used, it will be possible to achieve a high tolerance to thermal disturbances. The differences in the spin detection technologies between spin FET and quantum dot are the operation temperature, number of spins, and the amount of injection/detection current. Therefore, in this study, we investigated the applicability of the ferromagnetic tunnel contacts to the quantum technology.

Since the injected current is very small (0.5~50 μA), superimposition of spurious signals such as anisotropic magnetoresistance is inevitable in the MR measurements involving magnetization reversal. Therefore, the three-terminal Hanle measurement was employed, which does not require the magnetization reversal. In this measurements, a current is applied between two ferromagnetic tunneling contacts, and a voltage drop is detected only at the electrode under the spin extraction. The measurement was carried out at 30 K, because the carrier freezes out was taken place below 20 K.

The results for I = 50 and 2 μA, more than two-orders of magnitude smaller than that of typical value in spin FET, are shown in Fig. 1. The results were obtained by subtracting the signal of the parallel configuration from the that of the anti-parallel configuration. A clear Hanle signal was obtained at I = 50 μA. For I = 2 μA, although the signal-to-noise ratio was poor, a Hanle signal was still recognized. Since the electrode size is 6.3 μm^2, detection of spin signal is expected to be possible even less than 1 nA, if the ferromagnetic tunneling electrode is fabricated to the size required for application to the quantum dot (approx. 50nm×50nm).

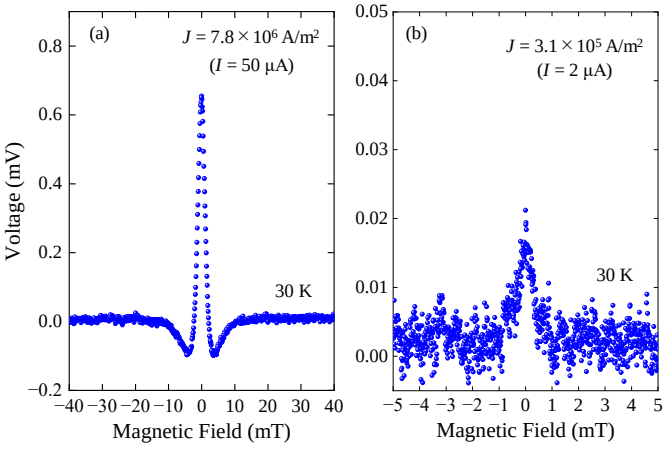

Figure 1 Difference in the three-terminal Hanle signal between the antiparallel and parallel configurations measured at 30K. Injection current is (a) 50 μA and (b) 2 μA, respectively.

[1] T. Tahara et al., Appl. Phys. Express. **8**, 113004(2015), [2] R. Ishihara et al., Phys. Rev. Appl. **13**, 044010(2020), [3] S. Sato et al., Phys. Rev. B **102**, 035305(2020), [4] K. Takeda et al., Nature **608**, 682 (2022). [5] J. Yoneda et al., Nat. Commun. **12**, 4114(2021).

Generation of highly spin-polarized electrons in Si at room temperature using low-resistance CoFe/Fe/Mg/MgO/n^+-Si junctions

○(B) Ryosuke Shimizu [1], Shoichi Sato[1, 2], Masaaki Tanaka[1, 2, 3], and Ryosho Nakane[1, 3, 4]
[1]EEIS, [2]CSRN, [3]NanoQuine, [4]d.lab, The University of Tokyo E-mail: koisuke@g.ecc.u-tokyo.ac.jp

Si-based spin metal-oxide-semiconductor field-effect transistors (spin MOSFETs), which use ferromagnetic metals as the source/drain electrodes, are promising for low-power electronics applications, such as reconfigurable logic circuits and high-density nonvolatile random-access memory, since their transistor characteristics can be programmed in a nonvolatile manner by the relative magnetization configuration between the source and drain ferromagnets [1]. The most crucial parameter is the magnetoresistance (MR) ratio that is proportional to P_S^2/R_T, where P_S is the spin polarization of tunneling electrons through a Si-based ferromagnetic tunnel junction and R_T is the total series resistance including the source and drain junction resistances R_J and the Si two-dimensional channel resistance [2]. Thus, Si-based ferromagnetic tunnel junctions with both high P_S and low R_J are essential for realizing high-performance spin MOSFETs toward practical use. However, such junctions have yet to be realized because of the trend in the relationship between P_S and R_J: higher P_S is mostly obtained with increasing resistance-area product (RA) [3]. This is the main reason why the MR ratio currently stands at only ~0.04% at room temperature [4].

It is known that P_S through a ferromagnetic tunnel junction is fundamentally limited by the spin polarization at the Fermi level of the ferromagnetic metal when the spin-filter effect of the tunneling barrier is absent. Hence, ferromagnetic materials with a high spin polarization are effective to enhance P_S. In this respect, CoFe is promising because CoFe has a higher spin polarization (~50%) than Fe (~45%) [5] that is frequently used for Si-based spin injection experiments. On the other hand, RA is related to the tunnel barrier layer in a Si-based ferromagnetic tunnel junction. So far, our experimental studies at room temperature revealed that Fe/Mg/MgO/n^+-Si has P_S = 7.3% and RA = 4 – 6 kΩμm^2 [2]. whereas Fe/Mg/SiO_xN_y/n^+-Si has P_S = 7.5% and RA = 0.7 kΩμm^2 [6]. Hence, SiO_xN_y or SiN is very useful to obtain lower RA, which is partly because a thin insulator tunnel barrier can be formed by direct oxi-nitridation or nitridation of Si surface with RF plasma. Here, we study ferromagnetic tunnel junctions with both a high P_S and a low R_J using CoFe and SiN, in which P_S is estimated from Hale signals measured with a three-terminal device and R_J is estimated from the I-V curve at around zero bias. Furthermore, we discuss the junction capability through a simple estimation of MR ratio using the device parameters in our previous spin MOSFET [2].

Figure 1 shows our three-terminal device structure having CoFe(10 nm)/Fe(0.7 nm)/Mg(0.5 nm)/SiN(1 nm)/n^+-Si tunnel junctions with 25 μm^2 in area and the measurement setup for Hanle signals at room temperature. The junction contains two interface-control layers; an Fe layer between Mg and CoFe to suppress Co interdiffusion [7] and a Mg layer between Fe and SiN to prevent interfacial reaction as well as to control the band alignment [6]. Figure 2 shows current density J versus junction bias voltage V, suggesting direct-tunneling-dominated transport. Figure 3 shows a Hanle signal measured with a constant current I_B = −10 mA in the spin extraction geometry, where red squares show experimental signal data and a black solid line shows a theoretical fitting curve [2]. After the analysis of Hanle signals obtained for three devices, the averaged P_S and RA values are 15.8% and 2.5 kΩμm^2, respectively. Then, the MR ratio was estimated using formulas in ref. [2], under the assumption that this junction is replaced with the source and drain of the spin MOSFET, where the Si two-dimensional inversion channel length and width are 0.4 μm and 180 μm, respectively, the gate oxide thickness is 200 nm, the source-to-gate voltage V_{GS} is 40 V, and the experimental junction characteristics in Figs. 2 and 3 are used. Since the P_S is increased and the MR ratio up to 0.76% is predicted, this junction structure has high potential for Si-based spin MOSFETs.

Acknowledgements: This work was partly supported by Grants-in-Aid for Scientific Research (20H05650, 23K17324, 23H00177) and Spintronics Research Network of Japan (Spin-RNJ).

References: [1] S. Sugahara and M. Tanaka, Appl. Phys. Lett. **84**, 2307 (2004). [2] S. Sato, et al., Phys. Rev. B **102**, 035305 (2020). [3] R. Nakane, et al., Phys. Rev. Mater. **3**, 024411(2019). [4] T. Sasaki, et al., Phys. Rev. Applied **2**, 034005 (2014). [5] S. V. Karthik, et al., J. Appl. Phys. **105**, 07C916 (2009). [6] R. Nakane, et al., Appl. Phys. Lett. **112**, 182404 (2018). [7] M. Yamada, et al., J. Appl. Phys. **129**, 183901 (2021).

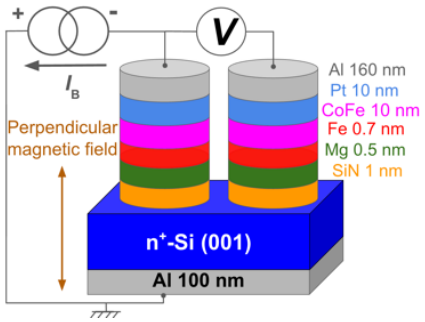

Fig.1 Schematic illustration of the device and three-terminal measurement setup.

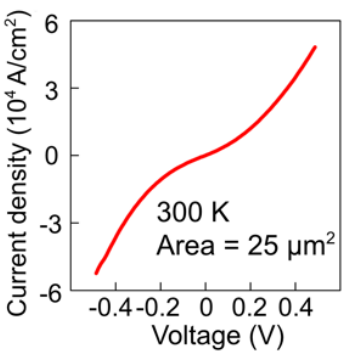

Fig.2 Current density J versus junction bias voltage V measured at 300 K.

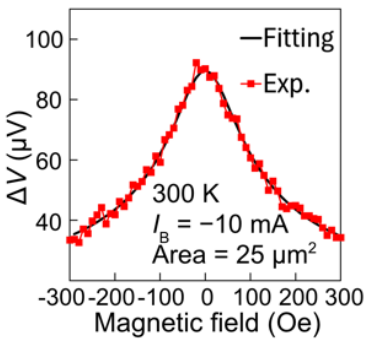

Fig. 3 Hanle signal measured at 300 K with a constant current I_B = -10 mA.

Optimized growth condition and quantum oscillation of topological semimetal Sb

Tomoki Hotta[1], Le Duc Anh[1,2], and Masaaki Tanaka[1,2]
[1]*Department of Electrical Engineering and Information Technology, The University of Tokyo*
[2]*Center for Spintronics Research Network (CSRN), The University of Tokyo*
E-mail: hotta@cryst.t.u-tokyo.ac.jp

Sb, a common element in III-V semiconductors, has been known to be topologically nontrivial since the early studies on topological materials [1]. To fully utilize its spintronic properties of topological surface states, high-quality epitaxial films are essential. Sb has a rhombohedral A7 crystal structure and can be epitaxially grown on the nearly lattice matched (111) surface of semiconductors whose lattice constant is close to 6.1 Å such as GaSb(111)A [2][3] and InAs(111)B [4] by molecular beam epitaxy (MBE). Recently we have developed epitaxial growth of Sb on GaSb(111)A [5], but the Sb thin films grown by this procedure have in-plane twin structures which degrade their transport properties. Here in this work, we optimize the MBE growth conditions for Sb on GaSb(111)A and observe Shubnikov-de Haas (SdH) oscillations originating from a hole pocket of the Sb Fermi surface, which is a signature of coherent quantum transport of the bulk carrier.

The studied sample structure consists of Sb (1 μm) / GaSb (100 nm) / GaSb(111)A substrate. The growth procedure for the GaSb buffer is the same as our previous report [5]. We varied the substrate temperature (T_{sub}) for Sb layer. When T_{sub} = 30°C, Sb becomes amorphous [5]. When $T_{sub} \geq$ 100°C, Sb grows as one-dimensional nanowires, which is consistent with the previous result [6]. When we grew Sb at T_{sub} = 60°C, reflection high energy electron diffraction (RHEED) patterns showed asymmetric streaks [upper panel of Fig. 1(a)], indicating epitaxial growth without twin structures. After the growth of 5-nm-thick Sb, the sample was annealed at T_{sub} = 260°C for 30 minutes. Finally, we grew 1-μm-thick Sb at T_{sub} = 200°C. RHEED patterns became much brighter with Kikuchi lines [lower panel of Fig. 1(a)], indicating successful epitaxial growth. We confirmed epitaxial relation of Sb(0003) // GaSb(111) from the out-of-plane X-ray diffraction (XRD) measurement [Fig. 1(b)], as expected.

At 300 K, magnetic-field-dependence of Hall resistance of our sample showed *p*-type conduction with a hole concentration of 1.02×10^{21} cm^{-3} and mobility of 205 cm^2/Vs, indicating that the Fermi level is located at a hole pocket. At 2 K, we observed giant positive magnetoresistance of about 100,000% and clear SdH oscillations [Fig. 1(c)]. Analysis of the SdH oscillations following the Lifshitz-Kosevich theory allows us to estimate the effective mass of $0.125m_0$, Berry phase of 0.825, and quantum mobility of 4460 cm^2/Vs of the observed Fermi surface. Frequency of the SdH oscillations becomes minimum when the magnetic field is tilted at about 60 degrees from perpendicular to the plane, which is consistent with the *k*-space structure of the Sb hole pocket [7]. These results demonstrate the high quality of our Sb thin film thanks to the optimized growth conditions and method.

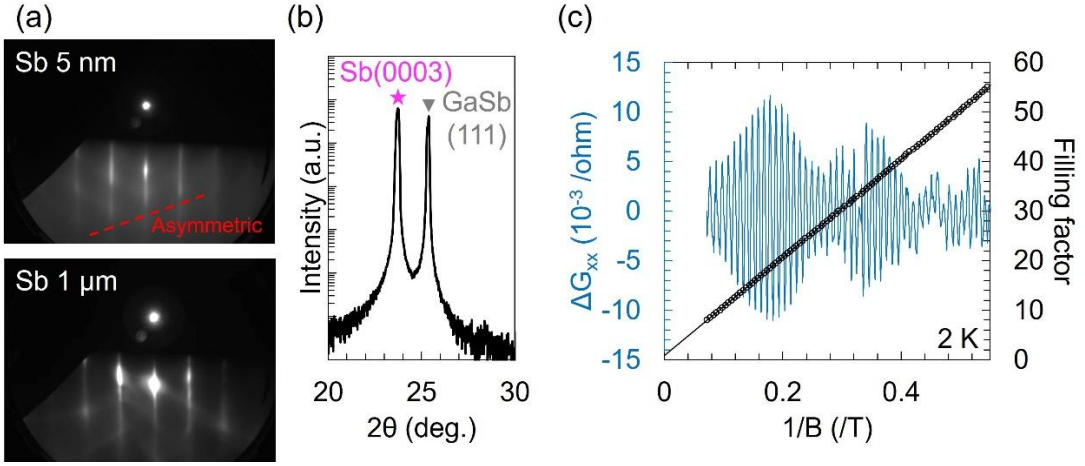

Figure 1 (a) RHEED patterns of a Sb thin film during the MBE growth. (b) Out-of-plane XRD spectrum of our Sb thin film sample. (c) Extracted SdH oscillatory component of longitudinal conductance ΔG_{xx} against inverse magnetic field (1/*B*) at 2 K. Black points are the filling factors at extrema of the oscillation.

References: [1] D. Hsieh, *et al*., Science **323**, 919 (2019). [2] J. A. Dura, *et al*., J. Appl. Phys. **77**, 21 (1995). [3] C. K. Gaspe, *et al*., J. Vac. Sci. Technol. B **31**, 03C129 (2013). [4] P. Mousley, *et al*., Phys. Status Solidi B **259**, 2100432 (2022). [5] T. Hotta, *et al*., The 71st JSAP Spring Meeting 2024, 25p-71B-6, Tokyo City University, March 25, 2024. [6] A. Proessdorf, *et al*., Nanotechnology **23**, 235301 (2012). [7] L. R. Windmiller, Phys. Rev. **149**, 472 (1966).

Effect of Pt and Bi on the spin Hall angle in topological semimetal YPtBi

[1] Institute of Science Tokyo, [2]Western Digital Inc., Great Oaks, [3]Western Digital Inc., Fujisawa
°Sho Kagami[1], Ohiro Fujie[1], Daiki Ito[1], Quang Le,[2] Brian York,[2] Cherngye Hwang,[2] Xiaoyong Liu,[2]
Son Le,[2] Maki Maeda,[3] Tuo Fan,[3] Yu Tao,[3] Hisashi Takano,[3] Pham Nam Hai[1]
E-mail: kagami.s.ad@m.titech.ac.jp

The half-Heusler topological semimetal YPtBi is a promising candidate for low power spin-orbit torque devices thanks to its relatively high spin Hall angle (>1) and high thermal budget (~600°C).[1)] The conductivity, spin Hall angle, and spin Hall conductivity of YPtBi are known to depend on the deposition condition, such as substrate temperature or Ar gas pressure,[2)] and stoichiometry.[3)] In this work, we study the fine tuning of Pt and Bi composition and reveal their role on the electrical and spintronic properties of YPtBi. We have deposited, from the bottom to the top, YPtBi (7 nm) / Pt (0.8 nm) / Co (0.8 nm) / Pt (0.8 nm) / $MgAl_2O_4$ (4nm) / Ta (1 nm) on sapphire substrates. Here, the YPtBi layer was deposited by co-sputtering Y, Pt, and Bi elemental targets at a substrate temperature of 400°C and an Ar pressure of 0.5 Pa. The Y deposition rate was fixed, but the Pt and Bi deposition rates were fine tuned. The Pt/Co/Pt trilayers were deposited at room temperature and they show perpendicular magnetic anisotropy. We used the second harmonic Hall measurement technique to evaluate the effective spin Hall angle θ_{SH}^{eff} of YPtBi in Hall bar devices. Figures 1(a)(b)(c) and 1(d)(e)(f) show the θ_{SH}^{eff}, conductivity σ_{YPtBi}, and effective spin Hall conductivity σ_{SH}^{eff} of YPtBi as functions of the Pt/Y and Bi/Y composition ratio, respectively. We observe that Pt has little effect on σ_{YPtBi}, but slightly increasing Pt/Y to about 1.1 can enhance both θ_{SH}^{eff} and σ_{SH}^{eff} significantly. This effect may be explained by the improved surface quality between YPtBi and Pt/Co/Pt trilayers, which in turn improves the interfacial spin transparency. Meanwhile, we observe that Bi has little effect on σ_{SH}^{eff}, but has large effect on σ_{YPtBi} and consequently, θ_{SH}^{eff}. This indicates that Bi is responsible for extra carriers in YPtBi. By tuning Bi/Y to about 1.1, we can reduce σ_{YPtBi} to 0.3×10^5 $\Omega^{-1}m^{-1}$ and maximize θ_{SH}^{eff} ~ 4.0. Our results provide a recipe for optimizing the spin Hall performance of YPtBi.

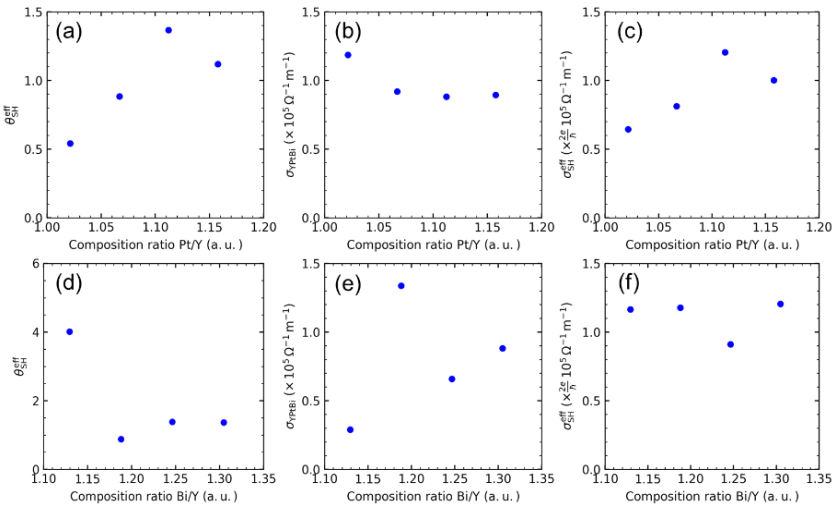

Fig. 1. (a)-(f) The dependence of (a), (d) the electrical conductivity of YPtBi (σ_{YPtBi}), (b), (e) the spin Hall angle (θ_{SH}^{eff}), (c), (f) the spin Hall conductivity (σ_{SH}^{eff}) on the compositional ratio of (a)-(c) Pt/Y at Bi/Y = 1.3 in YPtBi, (d)-(f) Bi/Y at Pt/Y =1.1 in YPtBi.

References

1) T. Shirokura, T. Fan, N.H.D. Khang, T. Kondo, P. N. Hai, Sci. Rep. **12**, 2426 (2022).
2) T. Shirokura and P.N. Hai, AIP Adv. **12**, 125116 (2022).
3) T. Shirokura, T. Kondo, P. N. Hai, Jpn. J. Appl. Phys. **61**, 073001 (2022).

Superconductivity of In-doped α-Sn thin films grown by molecular beam epitaxy

°Keidai Toyoshima[1], Hideki Maki[2], Le Duc Anh[1,2,3], and Masaaki Tanaka[1,2,3]
[1]*Department of Electrical and Electronic Engineering, The University of Tokyo*
[2]*Department of Electrical Engineering and Information Systems, The University of Tokyo*
[3]*Center for Spintronics Research Network (CSRN), The University of Tokyo*
E-mail: toyoshima-keidai@g.ecc.u-tokyo.ac.jp

Elemental α-Sn, with a diamond-type crystal structure, is expected to be a promising platform for topological physics, because it can be transformed to various topological phases. Under in-plane compressive strain, α-Sn thin films are topological Dirac semimetals (TDS) [1]. Furthermore, theoretical studies suggested that TDSs with superconductivity are topological superconductors which can host Majorana zero mode [2]. Recently, our group reported that α-Sn grown on an InSb substrate exhibited superconductivity 20 months after growth [3], probably originating from the doping effect when indium (In) atoms are diffused from the InSb buffer layer into the overgrown α-Sn thin film. This suggests a path to realize superconductivity in TDS α-Sn films by In-doping.

In this work, to develop a more controllable method, we grew 30nm-thick In-doped α-Sn films with In concentrations of 0.6, 1.8, 3, 5, 8.5 and 12.5% on InSb (001) substrates by molecular beam epitaxy. The crystal quality and surface roughness of the In-doped α-Sn films were characterized by *in situ* reflection high energy electron diffraction (RHEED) and X-ray diffraction (Fig. 1(a)). Zero resistance was observed in the samples with In-doping concentrations of more than 5% In (Fig. 1(b)), where the superconducting transition temperature (T_C) increased with increasing the In concentration. We measured the critical magnetic field H_C and critical current I_C under various magnetic field directions (Fig. 2). In-plane angular dependences of H_C and I_C were found to show sharp peaks when the magnetic field and the current are parallel. In addition, H_C was maximized when the magnetic field is perpendicular to the current. These angular dependences of superconducting properties are unique to In-doped Sn and suggest a contribution of TDS α-Sn to the superconductivity observed in the In-doped α-Sn thin films.

This work was partly supported by Grants-in-Aid for Scientific Research, CREST Program, and Spintronics Research Network of Japan (Spin-RNJ).

[1] L. D. Anh, et al., Adv. Mater. **33**, 2104645 (2021). [2] S. Kobayashi and M. Sato, Phys. Rev. Lett **115**, 187001 (2015). [3] T. Hotta, et al., 84th JSAP Autumn Meeting, 20p-C501-7, Kumamoto, September 2023.

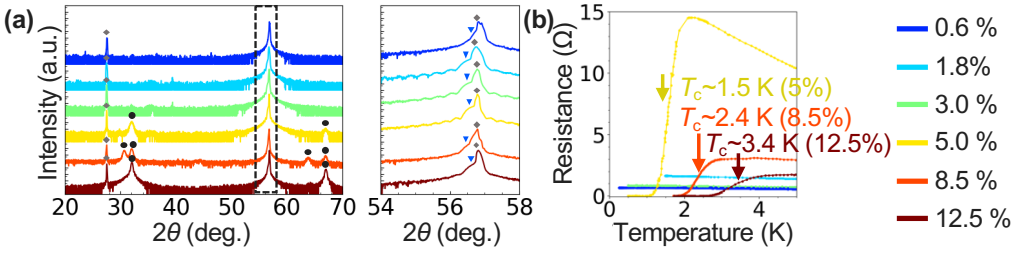

Fig. 1 (a) X-ray diffraction of the 30 nm-thick In-doped α-Sn films grown on InSb (001) substrates. Blue triangles, black circles, and gray squares are the peaks of α-Sn, β-Sn and InSb, respectively. Peaks of α-Sn were observed at all In-doping concentrations. (b) Temperature dependence of the resistance. Zero resistance was observed in samples with In-doping concentrations of more than 5%.

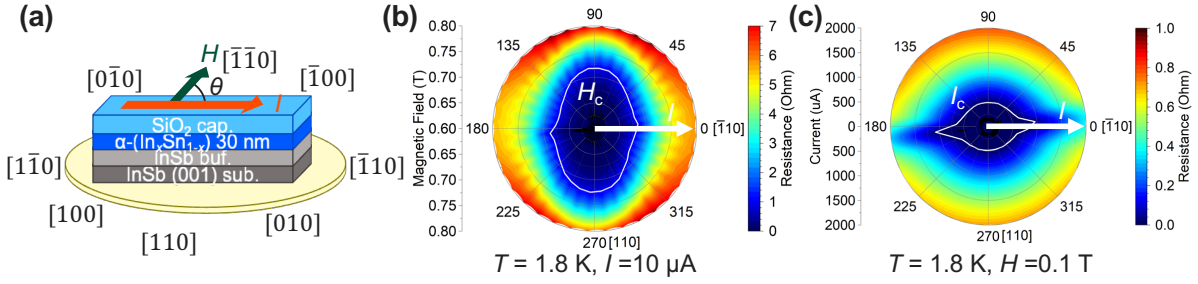

Fig. 2 Angular dependence of the critical magnetic field H_C and critical current I_C of In 12.5% doped α-Sn at 1.8K. (a) Schematic sample structure and measurement conditions. (b) Angular dependence of H_C at 10 μA. (c) Angular dependence of I_C at 0.1 T.

層状超伝導体 FeSe における磁場に無依存な超伝導ダイオード効果の詳細な特性評価

Detailed investigation of field-free superconducting diode effect in layered superconductor FeSe

京大工 [1]，京大 CSRN[2]，京大理 [3]
○(M)永田 歌寧 [1]，大同 暁人 [2,3]，大島 諒 [1,2]，柳瀬 陽一 [2,3]，白石 誠司 [1,2]
Dept. of Engineering, Kyoto Univ.[1], CSRN Kyoto Univ.[2], Dept. of Science, Kyoto Univ.[3]
○Utane Nagata[1], Akito Daido[2,3], Ryo Ohshima[1,2], Youichi Yanase[2,3], Masashi Shiraishi[1,2]
E-mail: nagata.utane.82w@st.kyoto-u.ac.jp

Superconducting diode effect (SDE) is a phenomenon [1], where nonreciprocal supercurrent flow takes place, has been intensively investigated from both experimental and theoretical approaches in spintronics as a novel physical effect. Meanwhile, the underlying physics is still elusive, and especially, the role of time-reversal symmetry is under debate [2]. Recently, SDE is observed without magnetic field in layered superconductor FeSe [3], of which origin is elucidated to be the interplay of thermal gradient originated from the Joule heating at contact resistances between FeSe and electrodes and an asymmetric geometry of FeSe.

In this study, we conducted detailed investigations to support the underlying physics we claimed. We experimentally investigated the influence of the geometry/edge effects and the relationship between the polarity of the SDE and the thermal gradient in the device. Figure 1 shows a measurement setup and the fabricated device. The FeSe was exfoliated on a thermally oxidized Si substrate, and the Au electrodes and Al heating wire were fabricated. The *I-V* characteristics were measured by the 4-terminal measurement and a diode efficiency η, defined as the difference of positive and negative critical currents divided by the sum of both critical currents, was estimated with changing the magnitude of the I_{heat} for providing external heat gradient control. Without the I_{heat}, electrode 2 side gets warmer because contact area is smaller, and the zero-field SDE (non-zero η) was observed as in our previous study [3]. When large I_{heat} is injected, electrode 1 side gets warmer and η is expected to be reversed. Figure 2 shows the I_{heat} dependence of η at 6 K. The polarity of the SDE efficiency was reversed when I_{heat} = 25 mA as expected, which directly indicates that the origin of this effect is the thermal gradient in the FeSe device, and more importantly, the SDE we discovered is the intrinsic effect. The detailed information will be introduced in the presentation.

Acknowledgement
We would like to thank Profs. Y. Matsuda, Y. Kasahara and S. Kasahara for their fruitful discussion.

[1] F. Ando *et al.*, Nature **584**, 373 (2020). [2] H.Wu *et al.*, Nature 604, 653 (2022).
[3] U. Nagata, M. Shiraishi *et al.*, under review (https://arxiv.org/abs/2409.01715).

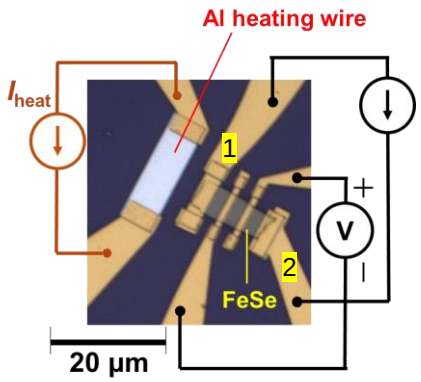

Fig. 1. An optical image of the fabricated device and a schematic of measurement setup

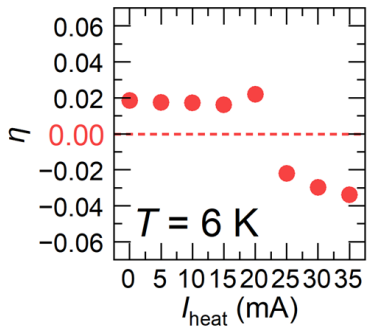

Fig. 2. I_{heat} dependence of diode efficiency η